# Information theory-based measures and privacy-preserving file formats for sensitive information leakage from raw functional genomics data

GG et al

March 23, 2018

## Abstract

Functional genomics experiments on human subjects present a privacy conundrum. On one hand, many of the conclusions we infer from these experiments are not tied to identity of individuals but represent universal statements about disease and developmental stages. On the other hand, by virtue of the experimental procedures, the reads from them are tagged with small bits of patients' variant information, which presents privacy challenges, as far as sharing the data. There is great desire to share the data as broadly as possible. Therefore it is useful to measure the amount of variant information leaked in a variety of experiments particularly in relation to the amount of sequencing. This allows to understand if there are ways of reducing the information leakage, and setting an appropriate setpoint for sharing information with only a small amount of leakage. To this end, we endevaour to address these problems here by deriving information theoretic measures for the private information leaked in experiments and developing various file format mnipulations for reducing much of the leaked variants.We showed that high depth experiments such as Hi-C provide accurate genotyping that lead to large privacy leaks. Counter intuitively, noisy and partial genotypes from low depth experiments such as ChIP-Seq and single-cell RNA-Seq, while not useful genotypes, can be used as strong quasi-identifiers for re-identification purposes through linking attacks. We showed that these incomplete genotypes can further be used to construct an individual's complete variant set and inference of individual identifying phenotypes when combined with imputation. We then provide a proof-of-concept theoretical framework, in which the amount of leaked information can be estimated from depth and breadth of the coverage as well as the sequencing bias of the functional genomics experiments. In order to solve the dilemma between data sharing vs. privacy leak, we propose a file formatting system that enables sharing of large amount of data while protecting individuals sensitive information and preserving the utility of the data. Such file format manipulation can be used in different levels to achive different levels of privacy and utility balance, hence provides a differential-privacy-like framework. At the highest level of privacy, our file-format masks all the variant information leaked from reads, which can be used to calculate signal profiles with 99% recovery of the original profiles and 100% recovery of

the original gene expression levels.

# 1 Introduction

With the decreasing cost of DNA sequencing technologies, the number and the size of the available genomic data have exponentially increased and become available to a wider group of audiences such as hospitals, research institutions and individuals [1]. In turn, privacy of individuals has become an important aspect of biomedical data science [2, 3] as availability of genetic information gives rise to privacy concerns such that genetic predisposition to diseases may bias insurance companies or create unlawful discrimination by employers [4].

Early genomic privacy studies focused on identification of individuals in a mixture by using phenotype-genotype association [5, 6]. These revealed that private information of an individual such as participation to a drug-abuse study can be revealed [5, 6]. With the increase of large-scale genomic projects such as Personal Genome Project (PGP) [7] or recreational/direct-to-consumer genomic databases, researchers showed that multiple datasets can be linked together to infer sensitive information such as pariticipant's surnames [8] or addresses [9]. Such cross-referencing relies on quasi-identifiers, which are pieces of information that are not unique identifiers by themselves, but are well correlated with unique identifiers or can be unique identifiers when combined with other quasi-identifiers [10].

Functional genomics experiments provide a wealth of information on genomic activities related to developmental stages or diseases that are essential for personilized medicine. These are large-scale, high-throughput assays to quantify transcription (RNA-Seq) [11], epigenetic regulation (ChIP-Seq) [12] or 3D organization of genome (Hi-C) [13] in a genome-wide fashion under different conditions (e.g. samples from patients and healthy individuals). Inferring biological information from functional genomics experiments is a several steps procedure, in which progresive summarization of the data from raw sequencing reads to the gene quantifications, TF binding peaks or chromatin interaction matrices is performed. Although activities of functional genome are not necessarily tied to an individual's genotype, reads from these experiments are derived from the biosamples that are belong to individuals, hence they are tagged with individual's variants. Public sharing of such raw data raises privacy concerns. To be able to share high utility data while preserving individuals' sensitive information, it is essential to determine a ''set point", after which trade-off between the utility of the data and the privacy risk is balanced. A hurdle in determining the 'set point" is the lack of systematic quantification of private information leakage from functional genomics data. Figure 1 summarizes the processing steps of RNA-Seq experiments as an example with how summarization decreases the risk of privacy while greatly decreasing the amount of sharing and the utility of the functional genomics data. In detail, functional genomics data analysis starts with the generation of DNA/RNA sequencing reads that are stored in special file formats called fastq [14]. These files are large in size ranging from 5 GB up to 60 GB depending on the purpose of the experiment. They are then mapped to human reference genome and these mapped reads are stored in compressed binary file types called SAM and/or BAM [15]. File formats such as CRAM is developed to remedy the ever increasing amount of data, which provides up to 10 fold decrease when information loss is tolerated [16]. Further summarization of the mapped reads (such as signal profiles or gene expression quantification) still allows researchers to make accurate biological conclusions, while providing further data reduction of a $\sim$20 fold. Although overall aggregation and averaging reduces biological information, private information leakage also decreases (Figure 1).

In particular, read alignment files (SAM / BAM / CRAM) are of great interest due to the large amount of biological data they provide as they constitute the most important input of majority of genome annotation pipelines. On the other hand, these files contain sequence information of the individual that may leak sensitive data. Depending on the depth of the functional genomics experiment, raw reads can be used to identify the private SNPs, small indels, and structural variants. However, current policies related to public sharing of the BAM files are somewhat ad-hoc. For example, for the genome of HeLa cell line, the raw reads from Hi-C experiments require special access, while reads from ChIP-Seq and RNA-Seq experiments are publicly available [17]. That is, reads from the experiments that do not require substantial depth are sometimes considered to be safe to share without privacy concerns owing to partial and biased sequencing, although it is not clear if these reads are leakage free. Although private information leakage from summary level functional genomics data are quantified previously [18, **?**, **?**] the lack of a systematic quantification of private data leakage from BAM files makes it difficult for biomedical data sharing policy makers to protect individual's sensitive information in a consistent fashion. CRAM format provides options for the users to convert BAM files into lossy compression, in which quality scores of the alignments are manipulated, which in turn can be used to decrease private information leakage [16]. However, there is still privacy leaks due to the containement of mismatch information of the reads with respect to reference genome [16]. MRF was introduced as a conceptual format to remedy privacy concerns, where keeping the sequence of reads is optional [21]. This does not only reduces the size of the data, but also makes it hard to genotype the individuals from the information in these files. However, private information leak is not entirely removed from MRF files, as one can still infer deletions from the information in these files. Moreover, current quantification pipelines used for gene expression analysis as well as the peak calling softwares were not designed to take MRF file format as inputs.

On the flip side of the coin is the utility of the mapped reads (BAM files) and challenges related to dealing with private data. Accession to private data requires use agreements that have expiration dates and a tremendous amount of bureaucracy connected to it. Moreover, any secondary data product becomes private and cannot be distributed. Problems associated with the distribution of secondary data products from private biomedical data is exacerbated due to large file sizes. For example, genome annotations that are derived from private functional genomics data require establishment of their own databases. However, since such annotations are derived from private data, establishment and distribution of these databases require extra levels of privacy related bureaucracy. Another example to the challenges associated with private data is that big consortia such as ENCODE [22], TCGA [23] or GTEx [24] fund multiple research institutions and enable a collaborative working environment through dedicated phone calls and meetings. In turn, participants have to go through required access procedures with their institutions. Otherwise communication based on private data is prohibeted according to data use agreements. Moreover, when multiple institutions have required access to the same data, they still cannot exchange files with each other. These challanges create a bottleneck and hinder the progress of important biomedical findings. Open data helps the advancement of biomedical data science not only with the easy access to the data, but also helping with the speedy assesment of tools and methods and in turn reproducibility. Funding agencies and research organizations are increasingly supporting new means of data sharing and new requirements for making data publicly available while preserving the participant's privacy [25]. In an attempt to consider both sides of the coin, we ask the questions of how much information is enough information to identify individuals and how we can protect the sensitive information with minimum loss of utility in a publicly data sharing mode. To this end, we derive novel information theory-based measures and apply these measures to quantify the amount of leaked information in 24 functional genomic assays from ENCODE [22] at varying coverages. Based on our findings, we develop new file formats that allow the public sharing of read alignments of functional genomics experiments while protecting the sensitive information as well as minimizing the amount of private data that requires special access and storage. Our file format manupilation system achieves different levels of privacy vs. utility balance with an adjustable parameter.

In this study, we use NA12878 as a case example and her 1000 genomes genotypes as gold standard genotypes [26]. We sample reads from the sequencing data of functional genomics experiments at increasing coverages and detect SNVs and indels using Genome Analysis Toolkit (GATK) best practices recommendations [27, 28]. We propose a new metric for qantifying the amount of information that can be obtained from sequencing data with respect to the gold standard. We next present a simple and practical instantiation of a linking attack with the assumption of adversaries accesing increasing amount of the seqencing data. We show that individuals are vulnerable to identifications even at small coverages of sequencing data. We further show that with summation of reads from functional genomics experiments and imputation through linkeage disequilibrium, the leaked number of variants can reach the total number of variants in an indivudal's genome. We then provide a theoretical framework where the amount of leaked information can be estimated from depth and breadth of the coverage as well as the bias of the experiments. Finally, we focus on ways to publicly share alignment data without comprimizing individual's sensitive information. We propose privacy enhancing file formats that hide variant information, are compressed and have minimum amount of utility loss.

# 2 Results

## 2.1 Information Theory to quantify private information in an individual's genome

An individual's genome can be represented as a set of variants. Each variant is composed of the chromosome it belongs to, location on that chromosome, the alternative allele and its corresponding genotype. Let $S = \{s_1, s_2, .., s_i, ..s_N\}$ be the set of variants, then each variant can be represented as $s_i = \{v_i, g_i\}$, where $v_i$ consists of the location and alternative allele information and $g_i$ denotes the genotype of the variant as 1 for heterozygous variant and 2 for homozygous variant. We can then calculate the naive self-information of $S$ in bits as

$$h(S) = -\sum_{i=1}^{i=N} log_2(p(s_i)). \tag{1}$$

In eq. 1, $N$ is the total number of variants in an individual's genome, $p(s_i) = n_i/n_T$ is the genotype frequency, in which $n_i$ is the number of individuals with variant $s_i = \{v_i, g_i\}$ and $n_T$ is the total number of individuals in the panel. Note that we denote $h(S)$ as "naive" information, because it is an estimate of the real information in a situation, which the population that the individual belongs to is not known and the number of inidivuals are finite. Eq.1 holds only if variants are independent of each other, which is not the case due to the correlation between variants in linkage disequilibrium (LD). In theory, the population that the individual belongs to can easily be predicted by using a few variants. However, from an adversary's perspective, this will add one more layer of calculation, i.e computational and time cost to identification attack. Eq.1 also an estimate to the information when we consider all the individuals in the world (i.e $\lim_{n_t \to \infty} h(S)$).

To be able to understand whether naive information is a good estimate, we first calculate the information with the consideration of LD scores taken from the European population of HapMap project [29]. LD scores are pairwise correlations between variants, which we consider as the prior information on the existence of a variant given other variants in the same LD block exist in a genome. Then the information with LD consideration is calculated as

$$h^{LD}(S) = -\sum_{i=1}^{i=N} (1 - mLD(s_i, s_j))h(s_i) \tag{2}$$

$LD(s_i, s_j)$ is the maximum LD correlation of variant $s_i$ such that $mLD(s_i, s_j) = \max_{i \neq j, j \in (1,..,N)} LD(s_i, s_j)$, where $mLD(s_i, s_j) \neq mLD(s_j, s_i)$.

Figure 2a shows a negligible difference between the naive information and information with LD consideration for NA12878 genome. To understand the lack of difference better, we calculate the self-information of each variant in an LD block with and without LD consideration. We show that highly informative variants do not exhibit any difference due to the low LD correlations (Figure 2b). We further show that the number of variants that have difference between information with and without LD consideration is small compared to highly informative variants having low LD correlations on average.

We then estimate the information when the population size is infinite [30]. We sample fractions in the order of 10%, 20%,..., 100% individuals from the 1000 genomes phase I panel (total of 2504 individuals) and calculate the information using the sampled distribution of genotypes. We repeat this calculation for 100 times and calculate the mean information for each sampled fraction. The relationship between the inverse of the sample fraction and the information fits best to a power function with two terms ($y = ax^b + c$, $R = 0.99$). The $y$-intercept ($c$) of the curve is the extrapolation of information when the population size goes to infinity ($1/\infty = 0$, Figure 2c). We again found a negligible difference between the naive information and the information when the population size is infinite (Figure 2a). The information is also calculated by starting from a single individual and adding individuls one by one to the population (SI Figure 1). These individuals are simulated using the genotype frequencies in the 1000 genomes panel and the LD information from HapMap project (see SI methods). Both the information calculation and the $KL$-divergence between different size populations show that as the size of the population increases, the difference in the information decreases and eventually becomes negligible (SI Figure 1)

In summary, calculations above show that the naive information can be an accurate approximate to the private information content of an individal's genome when the individual's population is not known and the population size is bound by the number of individuals in 1000 genomes panel due to the relationship of information at $n \to \infty \geq$ naive information $\geq$ information with LD (Figure 2a). That is, an adversary with no prior knowledge on the population of the sample and limited number of individuals in a known genotype panel can accurately approximate the private information in the sample.

## 2.2 Information Theory to quantify private information leakage in functional genomics data

In an effort to understand the relationship between the leaked information and the coverage as well as for a fair comparison, $k$ amount of reads were sampled from the 24 different functional genomic experiments and from WGS and WES data of NA12878 (see SI Table 1). Genome Analysis Tool Kit (GATK) is used to call SNVs and indels with the parameters and filtering suggested in GATK best practices [27, 28]. The genotypes in 1000 genomes panel for NA1278 is used as the gold standard. We use "naive" pointwise mutual information (pmi) as a measure to quantify the association between the gold standard and the called variants. If $S^G = \{s_1^*,..,s_i^*,...,s_M^*\}$ is the set of variants from the gold standard and $S^F(k) = \{s_1,..,s_i,...,s_M\}$ is the set of variants called from the $k$ total sequencing coverage of a functional genomics experiment, then the set $A = S^G \bigcap S^F(k)$ contains the variants that are called and are in the gold standard set. If $A = \{a_1,..,a_i,..,a_T\}$, then

$$pmi(S^G;S^F(k)) = -\sum_{i=1}^{i=T} log_2(p(a_i)) \tag{3}$$

We then add more reads to the sampled reads and repeat the calculation. This procudere is repeated till we deplete all the reads of a functional genomics experiment. The overall process is depicted in Figure 2e.

## 2.3 Private information leakage in 24 functional genomics experiment at different coverages

The pmi values for 24 functional genomics experiments are calculated at different coverages. These experiments involve whole genome approaches such as Hi-C, transcriptome-wide assays such as RNA-Seq and targeted assays such as ChIP-Seq of histone modifications and transcription factor binding. In addition, the pmi is also calculated for WGS, WES, and SNP-ChIP for comparison (Figure 3).

As expected Hi-C data contains almost as much information as WGS and more information than SNP ChIP arrays. WGS data contains more information than Hi-C in the beginning of the sampling process. As we sample nucleotides that are between around 1.1 and 10 billion bps, the information content of Hi-C surpasses the WGS data (Figure 3a). We speculate that this is due to better genotyping quality of the genomics regions that are in spatial proximity, as Hi-C has a bias of sequencing more reads from those regions. As expected, we cannot infer as much information from ChIP-Seq reads (Figure 3b). However, surprisingly many of the ChIP-Seq assays such as the ones targeting CTCF and RNAPII contain a great amount of information at low coverages. Furthermore, comparison between WES and different RNA-Seq experiments show that none of the RNA-Seq experiments contain as much information as WES, which is due to the fact that RNA-Seq captures reads only from expressed genes in a given cell (Figure 3c). The unexpected observation is that more information can be inferred from polyA RNA-Seq data at low coverages compared to WES and total RNA-Seq. To be able to make a fair comparison between all these assays, we calculate the mean pointwise mutual information per bp depicted in Figure 3d. To do so, we normalized the pmi values by the amount of coverage ($k$). We then averaged it by the number of times ($n$) we performed sampling on that experiment ($\frac{\sum pmi(S^F(k);S^G)/k}{n}$). We found that Hi-C experiments and ChIP-Seq experiments targeting the transcription factor HDGF provide more genotyping information per basepair compared to WGS data (Figure 3d).

## 2.4 Genotyping accuracy

In light of the above findings, in which genotyping can be done using low depth, biased functional genomics experiments, we asses the accuracy of genotyping by calculating the false discovery rate at different coverages. This also measures how much noise that each assay captures. The false discovery rate is defined as the ratio between the information obtained from the incorrectly called variants ($h(S^F \mid S^G)$) and the information obtained from all the called variants ($h(S^F)$), namely

$$FDR(S^F(k)) = h(S^F(k) \mid S^G)/h(S^F(k)) \tag{4}$$

Figure 4a shows that the false discovery rate for Hi-C data is lower compared to WGS data at lower coverages. We attribute it to the deeper sequencing of the genomics regions in close spatial proximity. Hence, sampling more reads from those regions at low coverages is more likely compared to uniform sampling of reads from WGS. ChIP-Seq data has comparable false discovery rate to WGS and Hi-C data, ChIP-Seq targeting CTCF having the lowest FDR (Figure 4b). We further find that assays targeting transcriptome such as WES and RNA-Seq produce the noisest genotypes among all the assays, only around 10% of the called variants being the correctly called variants (Figure 4c).

## 2.5 Linking attack scenario

Linking attacks aim at re-identification of an individual by cross-referencing datasets (Figure 5a). For example, in an hyphotetical scenario, the attacker aims at querying an individual's HIV status from his/her phenotype data. This phenotype data is released with the individuals' genotype information with an anonymized identifier for each individual. We assume that adversary obtains access to this dataset either lawful or unlawful means. Now let's assume that attacker has access to a biosample. This could be partial or complete mapped reads from functional genomics experiments or a saliva sample taken from a used glass. The idea is to do genotyping to the biosample and find the matching genotype in the HIV status database. However, individuals share many common variants with each other. The number of shared variants between individuals is large within a racial population and even larger within a family. Then the question becomes how well an adversary has to sequence an individual's genome to be able to do succesful linking. Specifically, adversary is interested in investigating whether noisy and partial reads from functional genomics experiments can be used as quasi-identifiers and how accurate the genotyping need to be in order to link individuals to databases.

For this, the attacker calls variants directly from the reads of anonymized functional genomic experiments. Then he/she compares the called noisy and incomplete genotypes to the genotype data panel and finds the entry with the highest pointwise mutual information. This reveals the sensitive information for the linked indivudal to the attacker. We then consider a scenario that the attacker has access partial or increasing amount of reads to find out when the data crosses the set point and becomes private.

Based on the pmi values of each experiment at different coverages, we define a metric for linking accuracy called $gap_{query}$. Let assume $S_i^{DB}$ is the set of variants that belongs to the $i^{th}$ individual in the genotype panel and $S^F_{query}(k)$ is the set of variants that was called from the functional genomics experiments of the query individual at $k$ total sequencing coverage. We first calculate the pointwise mutual information between every individual in the panel and the query as $pmi(S^F(k);S_i^{DB})$. We then ranked all the pmi values in a decreasing order such that;

$$pmi(S^F(k);S_i^{DB})^{(1)} > pmi(S^F(k);S_j^{DB})^{(2)} > ... > pmi(S^F(k);S_m^{DB})^{(N)}$$

In a real linking attack, the assumption is that individual with the highest pmi with the query $(pmi(S^F(k);S_i^{DB})^{(1)}$ is the query. Since our query individual (NA12878) is in the panel, we can measure the accuracy of this prediction with $gap_{query}$. We calculate the $gap_{query}$ for three possibilities: (1) First ranked individual is NA12878, (2) first ranked individual is not NA12878, but NA12878 is in the first five ranked individuals, and (3) none of the top 5 mathing individuals are NA12878. In the possibility (1), the attacker makes a correct prediction. The strength of this prediction is the $gap_{query}$, which is measured as the fold change difference between the pmi of best matching individual (coorect prediction) and the second best matching individual. In the possibility (2), the attacker makes a false prediction, but it can be correct if auxilary information such as gender and ethnicity is used. The strength of this prediction ($gap_{query}$) is measured as the fold change difference between the pmi of the real individual, that is ranked somewhere between $2^{nd}$ to $5^{th}$ and the pmi of the best matching individual, that is the misprediction. In the possibility (3), the attacker makes a false prediction that the query cannot be retrieved from the panel, there $gap_{query}$ becomes 0. We can formulate this as;

$$\begin{aligned}
&gap_{query} = \frac{pmi(S^F(k);S_i^{DB})^{(t)}}{pmi(S^F(k);S_j^{DB})^{(2)}}, \text{ if } S_i^{DB} = \text{query and } t = 1 \\
&gap_{query} = \frac{pmi(S^F(k);S_i^{DB})^{(t)}}{pmi(S^F(k);S_j^{DB})^{(1)}}, \text{ if } S_i^{DB} = \text{query and } t \in 2,3,4,5 \\
&gap_{query} = 0, \text{ otherwise}
\end{aligned} \tag{5}$$

We then define that if $gap_{query}$ is 0, then the individual cannot be identified as there are other individuals in the panel that have the matching genotypes. If $0 < gap_{query} \leq 1$, then the individual might be vulnerable with auxilary data such as gender or ethnicity, because he/she is in the top 5 macthing individuals. If $1 < gap_{query} \leq 2$, then the individual is vulnerable as we can identify him/her with 1 to 2 fold difference between him/her and the second best match. Lastly, if $gap_{query} > 2$, then the individual is extremely vulnerable with more than 2 fold difference between him/her and the second best match. Detailed flowchart of the linking attack is in Figure 5a).

We find that NA12878 is extremely vulnerable even at the lowest sampled coverages for Hi-C and RNA-Seq data (Figure 5b). More interestingly between around 1.1 and 10 billion basepairs, the Hi-C data exhibits higher linking accuracy than WGS data, consistent with the previous observation of pmi shown in Figure 3a. The total of coverage of ChIP-Seq data compared to Hi-C and RNA-Seq is quite low (SI Table I). However, the linking accuracy of ChIP-Seq is as good as Hi-C and WGS (Figure 5b), which shows extreme vulnerability of individuals with respect to release of such small amount of data. More strikingly, attacker can link NA12878 by using the reads of single-cell RNA-Seq data, which cover a small portion of the genome in a single cell (Figure 5d). We then added the variants of NA12878's parents to the 1000 genomes genotype panel and repeated the linking attack. We found that although NA12878 is still extremely vulnrebale to re-identification in the presence of her parents in the database, the second best matching individuals are her parents (SI Figure 2). This shows that using the metric *gap*, an adversary can also identify individuals related to the target individual.

## 2.6 Individual's genome can be accurately approximated from publicly available data by imputation

To answer the question whether an attacker can correctly assemble an individual's variants by only using the reads from ChIP-Seq and RNA-Seq experiments, we impute variants by using IMPUTE2 [31, 32, 33] and the variants called from ChIP-Seq and RNA-Seq experiments. We then collected all the called and imputed variants in a set. Although imputed variants do not contribute to the information due to high correlation with the called variants (SI Methods and SI Figure 3), total number of captured variants increases significantly (Figure 6a). By using shallow squencing data of ChIP-Seq and RNA-Seq, we were able to call and impute variants almost as many as the gold standard variants.

We then ask the question if we can infer potentially sensitive phenotypes from these variants. Figure 6b shows a small set of example variants associated with physical traits such as eye color, hair color or freckles. Many of these variants are in the called set of Hi-C, ChIP-Seq and RNA-Seq data. Number of variants associted with traits further increases with imputation as expected.

## 2.7 Toy model for estimation of amount of leaked data without variant calling

Genotyping from DNA sequences is the process of comparing the DNA sequence of an individial to that of reference human genome. To be able to do succesful genotyping, one needs substantial depth of sequencing reads for each base pair. According to the Lander-Waterman statistics for DNA sequencing, when random chunks of DNA is sequenced repeteadly, the depth per basepair follows Poisson distribution with a mean that can be estimated from the read length, number of reads and the length of the genome [34]. Since functional genomics experiments aim at finding highly expressed genes, TF binding enrichment or 3D interactions of the genome, it is expected that the sequencing depth per basepair does not follow the Poisson statistics. Thus, the genotyping using reads from functional genomics experiments is biased towards the variants that are in the functional regions of the cell types/lines of interest.

To this end, we hyphotesized that the genotyping from the sequencing based functional genomics data depends on the average depth per base pair ($\overline{d}$) , the total fraction of the genome that is represented at least by one read, also called the breadth ($b = \sum_{i=1}^{N} \delta(d_i)$, such that $\delta(d_i) = 1$ if $d_i > 0$, 0 otherwise and $N$ is the total number of nucleotides in the genome) and a parameter $\beta$ that estimates the sequencing bias, i.e. how much the distribution of depth per basepair deviates from the Poisson distribution (Fig. 6c). The bias parameter $\beta$ is composed of two terms: (1) the negative bias $\beta-$ and (2) the positive bias $\beta+$. Negative bias estimates if there is an increase in the number of low depth basepairs relative to mean with respect to espected Poisson distribution and the positive bias estimates the increase in the number of high depth basepairs (see SI for more details).

To quantify the genotyping accuracy from the functional genomics data, we used "naive" normalized pointwise mutual information (npmi). It takes into account the information from the correctly identified genotypes ($pmi(S^F;S^G)$), the information missed that is in the gold standard ($h(S^G \mid S^F)$) and the information from the incorrectly identified genotypes, i.e FDR ($h(S^F \mid S^G)$) as;

$$npmi(S^F;S^G) = \frac{pmi(S^F;S^G)}{h(S^F,S^G)} = \frac{pmi(S^F;S^G)}{h(S^G \mid S^F) + pmi(S^F;S^G) + h(S^F \mid S^G)} \tag{6}$$

To be able to get a fit for the relationship of $npmi(S^F;S^G) = f(\overline{d_F}, b_F, \beta_F)$, we used Gaussian Process Regression (GPR) [**?**] to fit 40 training data points and achieved a root mean square error (RMSE) of 0.06 with the values ranging between [0,35] (Fig. 6d). 5 separate data points were used as test set and an RMSE of 0.07 was acheieved (Fig. 6d), see SI for more details). The regression learning is performed using 10 fold cross-validation to protect against overfitting. This toy model represents a conceptual theoretical framework limited to the small sample space available. It shows that the amount of leaked data from functional genomics experiments can be estimated without the need of performing time-consuming genotyping calculation.

## 2.8 Unique combination of common variants contribute significantly to the information leakage and linking accuracy

We next analyze whether a linking attack can be prevented by removing rare variants from the datasets as their contribution to the information is the highest. We first speculated that the removal of the variants that are unique to NA12878 might be enough to fail at linking. A total of 11,472 variants along with their genotypes are only observed in NA12878, which we refer as ‘unique variants” (Fig. 6a). After the removal of unique variants from the NA12878 variant set, we calculated the $gap_{NA12878}$ and surprisingly found that linking accuracy is affected minimally compared to using the all of NA12878 variants (Fig. 6b). We then created another set (‘double variants”, Fig. 6a), that includes the variants that are observed in NA12878’s genome as well as one more individual in the 1000 genomes genotype panel (total of 16,305 genotypes). We again found that individual is extremely vulnerable to linking attacks ($gap_{NA12878} > 2$,Fig. 6b). We then relaxed our cut-off further to remove the variants that are observed in NA12878's genome as well as at most 1.5% of the population ('rare variants", total of 124,093 genotypes, Fig. 6a). This also did not affect the overall linking ($gap_{NA12878} > 2$,Fig. 6b).

These rare genotypes are observed in 64 or less individuals including NA12878. A practical solution to the re-identification problem using functional genomics data would be masking or removing such rare genotypes from the reads. However, as iteratively shown here that although rare variants are extremely informative and sufficient enough to do re-identification through linking attacks, their removal is not sufficient to fail at re-identification. That is, not only the rare genotypes but also the unique combination of common genotypes are identifiers of genetic make-up of an individual. To further support this calculation, we added the genotypes of the parents of NA12878 to the panel and found that we can still link NA12878 to the correct genotypes succesfully with an extreme vulnerability ($gap_{NA12878} > 2$, SI Fig. 2).

We then analyze the contribution of small indels to the naive information and whether accurate linking is possible when we remove all the single nucleotide mutations from the data and keep the indels. Fig. 6c shows the information contribution of the indels. Although naive pointwise mutual information from indels are much smaller compared to single nucleotide mutations, a high linking accuracy can be achived by using only indels even at small coverages (Fig. 6d). This linking attack is done using the most noisy data set we have (total RNA-Seq) to make linking more difficult.

## 2.9 Privacy-preserving file formats for alignments from functional genomics experiments and relation to *k*-anonimity

Sharing of raw alignments from functional genomics experiments are extremely important in developing analysis methods and discovering novel mechanisms about human genome. The purpose is to share maximum amount of information with minimum utility loss while largely maintaining the individual's privacy. As a privacy metric, we aim to prevent leakage of any variants as well as any quasi-identifier that can lead to identification of position of variants in the genome. We introduced a user identified privacy-utility balance that can be adjusted according to the patients' consents and institutions' policies. By using the concept of $k$-anonimity [**?**], we applied privacy-preserving transformation to the alignment files such that calling variants from transformed files are largely prevented while quantifications related to functional genome is possible with minimal error (Fig. 8a).

A release of data posesses the $k$-anonymity property if the information for each person contained in the release cannot be distinguished from at least $k-1$ individuals whose information also appear in the release. Although this concept was developed for the release of datasets with individuals, we can think of a raw alignment file (BAM) as a dataset, where information for each read is contained. Let's assume a BAM file is a dataset $D$, where each entry is a read. The desire is to release dataset $D$ in a form (say $D^*$) such that it does not leak variants from the reads, but in the mean time any calculation $f$ based on $D$ and $D^*$ retrieves almost the same result. There are two general methods to achieve $k$-anonimity for some value of $k$: suppression and generalization. If every column in $D$ is an attribute (such as read length, cigar, sequence, quality value), then replacing an attribute to an asteriks(*) is suppression, changing an attribute with a more general value is generalization. For example, in our file format transformation, we replace sequence and sequence quality attributes with asteriks (suppression), and transform the cigar of the read from partially mapped to fully mapped (generalization) to achive, for example,3-anonimity with respect to attributes sequence, sequence quality and cigar (see SI Methods for details). Now let's say the privacy-preserving transformation is done through a function $P_{Q,r}$ such that $P_{Q,r}(D) = D^*$. $Q$ is the operation such as ''removal of small indels", ''removal of mismatches", ''removal of large indels" or ''removal of all variants". $r$ is the amount of reads to be manupilated given the operation $Q$. A calculation $f$ can be signal depth profile calculation, TF binding peak detection or gene expression quantification (Fig. 8a). Then, we can reconstuct the eq. 7 for each unit $i$ as

$$\frac{f(D)}{f(D^*)} = e^{\varepsilon_i}, \tag{7}$$

where a unit can be a single basepair, an exon or a gene depending on the function $f$. In turn, $\varepsilon_i$ can be calculated as the log fold change between the results derived from two datasets. This is also a quantity commonly used to compute differential gene expression [37] or ChIP-Seq binding enrichment over controls [**?**], and can be used as analogous in this context, where log-fold change is the differential signal depth or expression when the manupilated data is used as an input.

Note that $\mid \varepsilon_i \mid$ is a measure of utility of the new dataset $D*$. We then calculated the distribution of $\mid \varepsilon_i \mid$ values over every unit and found the mean $\mid \varepsilon \mid$ per unit as the overall utiliy metric. The level of privacy is controlled by the function $P_{Q,r}$, where $Q$ determines the type of entries and $r$ determines the number of entries of given the operation $Q$ that are manipulated. For example, if $Q$ is the removal of indels and $r$ is the reads that contain indels with $MAF < 0.5$, then only reads that have indels with $MAF < 0.5$ will be manipulated in the transformed $D*$. In that case, adversaries cannot call indels using $D*$.

The privatized file format pBAM from data $D^*$ is constructed as following. The reads from the BAM files are categorized as perfectly mapped reads and reads with mismatches, insertions, deletions, soft- and hard-clipping. $P_{Q,r}$ replaces the sequence of all of the reads with asteriks and manipulates the cigars, alignment scores and the MD tags of the reads that are defined in $Q$ and $r$. The details of how new file format deals with reads are reported in SI Methods with a figure (SI Fig. 4). pBAM files can also be created from BAM files that are obtained by mapping sequences to the transcriptome coordinates, which is essential for gene quantification. Our transformation function $P_{Q,r}$ is general and can be applied to any alignment file types such as SAM, CRAM and MRF to create privatized new file format. These files will be concordant to use with tools such as samtools, cramtools and mrftools.

We calculated the signal depths of each basepairs in the genome using NA12878 RNA-Seq BAM file using STAR [**?**]. We then converted the BAM file into pBAMs with different $q$s and calculated the signal depth of each basepair. Fig. 8b shows the number of basepairs with $\varepsilon_i > 0$ with respect to number of basepairs with no change between BAM and pBAM. We did the same calculation by averaging signal over exons as well (Fig. 8b). Furthermore, we created pBAM files for the BAM files that are mapped on reference transcriptome and compared the gene quantification with the gene expression levels calculated from original BAM files. We used RSEM for gene quantification and STAR for transcriptome alignment [**?**, **?**]. We found no difference between the gene expression levels calculated using original BAM files and pBAM files (see Fig 8b and SI Methods for how we treated transcriptome alignments). Overall, when we remove all the variant leak from BAM files, we found 0.18% difference at the basepair resolution, 0.27% difference at the exon resolution, and 0% difference at the gene level. When we remove leak associated with the mismatches, we do not see any difference as when the cigars with mismathes are manipulated, the correct mapping locations can be recovered without leakage (see SI Methods). We when remove leak associated with indels, we found 0.0016% difference at the basepair resolution and 0.0011% at the exon resolution and 0% difference at the gene level. When we remove leak associated with split reads, we found 0.17% difference at the basepair resolution and 0.26% at the exon resolution and 0% difference at the gene level.

The pBAM file format contains necessary information to be used in functional genomics pipelines such as gene expression quantification and transcription factor binding peak calling. The difference between the results of ENCODE Chip-Seq TF binding peak calling pipeline (MACS2 [**?**]) is even more negligible when BAM and pBAM are used as input (SI Fig. 4). We then create a .diff file format that contains the original information that was manipulated in the pBAM file. With the motivation of keeping size of private file formats relatively small, we report only differences between BAM and pBAM in the .diff file by avoiding the printing any sequence information of the reads that can be found in the reference human genome (see SI Methods). diff files are private files that require special permission for access. A user is able to retrieve the original BAM file when they have access to the .diff file by using our collection of scripts called ptools that can convert pBAM + .diff + reference genome into the original BAM file (Fig 8c).

### 2.9.1 Implementation

Conversion of BAM files to pBAM and pBAM+diff files back to BAM files are implemented as a series of scripts in bash scripting language and python. Diff files are encoded in compressed format to save space. For convenience, pBAM files are saved as BAM files with manupilated content and saved with p.bam extension. That is, any pipeline that uses BAM as an input can take p.bam as an input as well. Running times and assiciated file sizes for alignemnts from RNA-Seq experiments and ChIP-Seq experiments is documented in Table x [[MEG to fill the table]]. Our file format manipulation is adopted by ENCODE Consortium Data Coordination Center. Codes for the calculation of information leakage, scripts for file manupilation as well as examples of BAM, pBAM and diff files can be found at privaseq3.gersteinlab.org.

Table 1: pTools performance

| Experiment | BAM size | q | $\varepsilon$ | pBAM size | .diff size | BAM to pBAM runtime | pBAM+diff+hg to BAM runtime |
|---|---|---|---|---|---|---|---|
| RNA-Seq genome | | | | | | | |
| RNA-Seq transcriptome | | | | | | | |
| ChIP-Seq CTCF | | | | | | | |
| ChIP-Seq H3Kme4 | | | | | | | |

# 3 Discussion

Functional genomics experiments provide large amount of biological data. These are large-scale, high-throughput assays based on sequencing. Although they aim at answering questions related to genomic activities such as gene expression, TF binding or 3D organization of genome, public sharing of sequencing data from these experiments can lead to recovery of genotype information and in turn raise privacy concerns. However, the systematic quantification of private information content of the functional genomics BAM files and open access to such data without comprimising individuals' identity have not been well studied. Current policies regarding to public sharing of functional genomics BAM files are ad-hoc. The experiments that require high depth of sequencing such as Hi-C and sometimes RNA-Seq are considered to be private, while relatively low depth BAM files such as those from ChIP-Seq are often shared publicly. In this study, we derived information theory based measures to systematically quantify the sensitive information leakage in the BAM files of functional genomics experiments in low and high depth experiments.

Instantiation of linking attacks by genotyping of partial or complete functional genomics data showed that even at low coverages of low depth experiments such as ChIP-Seq, linking individuals to the databases can be done without error. When we compare the linking accuracy to the false discovery rate, we found that it is easier to link individuals to the databases than genotyping them accurately using functional genomics experiments. The implication is that noisy quasi-identifers, i.e bad quality SNP calling, can be used to link the data to the high quality genotypes. For example, according to our calculations, reads from singel-cell RNA-Seq data carry the most amount of noise. This is likely due to the bias towards expressed genes in such small amount of cells, mapping issues of splice sites, false positives from RNA editing sites and amplification bias. However, the noisy genotypes called from small amount of cells, even when the number of reads are only a million, are quasy-identifiers that result in very high linking accuracy. This is worrisome in terms of biomedical data sharing as the number of individuals in genotype databases is increasing exponentially with the decrasing cost of sequencing. Furthermore, rich information about an individual's identity and his/her sensitive phenotypes can also be inferred by combining the reads from low depth functional genomics experiments and through genotype imputation.

In this study, we also discuss the concept of ''set point" in determining the data production steps, where sensitive information leakage and utility of the data are balanced (Fig. 1). Setting a ''set point" is possible by systematic genotyping and quantification of information. Although it is obvious that any DNA read contains variants, it is not trivial to understand the amount and the quality of sequencing to do accurate genotyping. Moreoever, we showed that genotyping accuracy of a functional genomics sample and the ability to link individuals to the databases using the same sample are not necessarily correlated. It is easier to link individuals to the databases and infer their complete variant sets than genotyping a sample with accuracy and minimal false discovery. For example, complete set of variants from HeLa's genome may not be obtained by genotyping HeLa BAM files from functional genomic experiments. However, using only a small number of reads from the same BAM files accurate linking attacks are plausable. That is, noisy and incomplete genotyping from partial sequencing experiments can serve as strong quasi-identifiers, which is not straightforward to predict at first. Nevertheless, policies governing public sharing of HeLa genome vs. HeLa functional genomics reads is ad-hoc and contradictory. Therefore, it is essential to quantify the information in samples and set the ''set point" accurately. On the other hand, functional genomics experiments advanced our undertsanding of health and disease by revealing function of the genome under different conditions. The quantification, analysis and the interpretation of functional genomics data are still an evolving field, hence extensive public sharing of functional genomics data accelerate collaborative research and reproducibility by removing the complexities associated with data accession procedures.

The increasing incentive to share data for the advancement of biomedical research and the correlated increrasing privacy concerns have led researchers to look for more complex solutions to overcome the bottleneck between data-sharing and privacy preserving means. Solutions such as differential privacy has been proposed [?, ?, ?]. It has shown that retriving summary information from private statistical databases without revealing some amount of individuals' information is impossible [?]. Furthermore, entire database can be inferred by using a small number of queries. Differential privacy ensures a high level of privacy such that adversary retrieves similar result with and without the addition of the individual's data to the database by adding perturbations or noise to the queries [?]. We further studied if the concept of differential privacy can be utilized to create leakage-free raw functional genomics data (see SI Methods). Although such concept is useful for sharing summary statistics of functional genomics data from multiple individuals, it is conceptually hard to apply to the raw mapped read sharing from functional genomics experiments taken from a single individual. While further research will be fruitful on how to extract useful information from genomics data that are noised and perturbed, we envision there will be more applications of privacy concepts such as differential privacy in genomics data sharing such as releasing population based genotype-phenotype data [36, ?] .

To enable public sharing of raw alignments from functional genomics experiment, we designed a privacy-preserving transformation and created privacy-preserving binary allignment files (pBAM). We developed a framework, where researchers can tune the level of privacy and utility balance they want to achieve based on the policies and consents of the donors. pBAMs enable researchers to share the mapped reads, which are largest data product of functional genomics experiments. To easen the challenges associated with moving and storing of large special access files, we created light-weight .diff file format that consists of the differences between pBAM and BAM files in a compact format. This allows us not to repeat the sequence information in the human reference genome files in .diff files and reduces the size of the private files significantly. Presented framework can be used for quantification of sensitive information from the raw reads of functional genomics experiments and conversion of raw files to privacy-preserving file formats. We address the most obvious leakage and provide solutions for quick quantification and safe data sharing. However, it is useful to review all the sources of information leakage from functional genomics experiments. For example, the next source of leakage is from the signal profiles in RNA-Seq, which was addressed elsewhere [20]. There is also leakage from gene expression quantifications, which was shown to be connected with variants through the eQTLS [19]. Quantification of the leakage in all levels of data processing steps of an RNA-Seq experiment is tabulated in Table 2 and in SI Fig. x. We also anticipate more leakages to be discovered as new functional genomics experiments are developed. Combined with the increasing attention to genomic privacy, we expect future studies will lead to novel privacy-preserving solutions in an open data sharing mode.

Table 2: Quantification of leakage in different sources

| Leaking source | Leaking variants | Average leakage per variants (bits) | Maximum leakage per variant (bits) | Total leakage (bits) |
|---|---|---|---|---|
| Raw reads | Exonic& Intronic variants | | | |
| RNA-Seq Signal profile | Exonic deletions | 0.196±0.311 | 5.525±0.311 | |
| Gene expression | eQTLs | 0.825±0.250 | 2.772±1.335 | |

# References

[1] Sboner A, Mu X, Greenbaum D, Auerbach RK, Gerstein MB. The real cost of sequencing: higher than you think! *Genome Biology*, 2011;12(8):125.

[2] Joly Y, Dyke SOM, Knoppers BM, Pastinen T. Are Data Sharing and Privacy Protection Mutually Exclusive? *Cell*, 2016;167(5):1150-1154.

[3] Erlich Y, Narayanan A. Routes for breaching and protecting genetic privacy. *Nat. Rev. Genet.*, 2014;15(6):409-421.

[4] Joly Y, Feze IN, Song L, Knoppers BM. Comparative Approaches to Genetic Discrimination: Chasing Shadows? *Trends Genet*, 2017;33(5):299-302.

[5] Homer N, Szelinger S, Redman M, Duggan D, Tembe W, Muehling J, Pearson JV, Stephan DA, Nelson SF, Craig DW. Resolving individuals contributing trace amounts of DNA to highly complex mixtures using high-density SNP genotyping microarrays. *PLoS Genet.*, 2008;4(8):e1000167.

[6] Im HK, Gamazon ER, Nicolae DL, Cox NJ. On sharing quantitative trait GWAS results in an era of multiple-omics data and the limits of genomic privacy. *Am. J. Hum. Genet.*, 2012;90(4):591-598.

[7] Church GM. ”The Personal Genome Project”. *Molecular Systems Biology*, 2005;1(1):E1E3.

[8] Gymrek M, McGuire AL, Golan D, Halperin E, Erlich Y. Identifying personal genomes by surname inference. *Science*, 2013;339(6117):321-324.

[9] Sweeney L. k-anonymity: a model for protecting privacy. *International Journal on Uncertainty, Fuzziness and Knowledge-based Systems*, 2002;10(5):557-570.

[10] Sweeney L. Simple demographics often identify people uniquely. *Carnegie Mellon University, unpublished*, 2000.

[11] Wang Z, Gerstein M, Snyder M. RNA-Seq: a revolutionary tool for transcriptomics. *Nat. Rev. Genet.*, 2009;10(1):57-63.

[12] Pepke S, Wold B, Mortazavi A. Computation for ChIP-seq and RNA-seq studies. *Nat. Rev. Genet.*, 2009;6:S22S32.

[13] Lieberman-Aiden E, van Berkum NL, Williams L, Imakaev M, Ragoczy T, Telling A, Amit I, Lajoie BR, Sabo PJ, Dorschner MO, Sandstrom R, Bernstein B, Bender MA, Groudine M,

Gnirke A, Stamatoyannopoulos J, Mirny LA, Lander ES, Dekker J. Comprehensive mapping of long-range interactions reveals folding principles of the human genome. *Science*, 2009;326(5950):289-293.

[14] Cock PJA, Fields CJ, Goto N, Heuer ML, Rice PM. The Sanger FASTQ file format for sequences with quality scores, and the Solexa/Illumina FASTQ variants. *Nucleic Acids Research*, 2009;38(6):1767-1771.

[15] Li H, Handsaker B, Wysoker A, Fennell T, Ruan J, Homer N, Marth G, Abecasis G, Durbin R. The Sequence Alignment/Map format and SAMtools. *Bioinformatics*, 2009;25(16):2078-2079.

[16] Hsi-Yang Fritz M, Leinonen R, Cochrane G, Birney E. Efficient storage of high throughput DNA sequencing data using reference-based compression. *Genome Res.*, 2011;21(5):734-740.

[17] Beskow LM. Lessons from HeLa Cells: The Ethics and Policy of Biospecimens. *Annu Rev Genomics Hum Genet.*, 2016;17:395-417

[18] Schadt EE, Woo S, Hao K. Bayesian method to predict individual SNP genotypes from gene expression data. *Science*, 2012;44(5):603-608.

[19] Harmanci A, Gerstein M. Quantification of private information leakage from phenotype-genotype data: linking attacks. *Nature Methods*, 2016;13(3):251-256.

[20] Harmanci A, Gerstein M. Analysis of Sensitive Information Leakage in Functional Genomics Signal Profiles through Genomic Deletions. *Nature Communications*, 2017

[21] Habegger L, Sboner A, Gianoulis TA, Rozowsky J, Agarwal A, Snyder M, Gerstein M. RSEQtools: a modular framework to analyze RNA-Seq data using compact, anonymized data summaries. *Bioinformatics*, 2011;27(2):281-283.

[22] ENCODE Project Consortium. An integrated encyclopedia of DNA elements in the human genome. *Nature*, 2012;489(7414):57-74.

[23] Cancer Genome Atlas Research Network, Weinstein JN, Collisson EA, Mills GB, Shaw KR, Ozenberger BA, Ellrott K, Shmulevich I, Sander C, Stuart JM. The Cancer Genome Atlas Pan-Cancer analysis project. *Nature Genetics*, 2013;45(10):1113-1120.

[24] The GTEx Consortium. The Genotype-Tissue Expression (GTEx) project. *Nature Genetics*, 2013;45(6):580-585.

[25] National Institute of Health data sharing policy. https://grants.nih.gov/grants/guide/notice-files/NOT-OD-17-110.html

[26] The 1000 Genomes Project Consortium. A map of human genome variation from population-scale sequencing. *Nature*, 2010;467(7319):1061-1073.

[27] DePristo M, Banks E, Poplin R, Garimella K, Maguire J, Hartl C, Philippakis A, del Angel G, Rivas MA, Hanna M, McKenna A, Fennell T, Kernytsky A, Sivachenko A, Cibulskis K, Gabriel S, Altshuler D, Daly M. A framework for variation discovery and genotyping using next-generation DNA sequencing data. *Nature Genetics*, 2011;43(5):491-498.

[28] Van der Auwera GA, Carneiro M, Hartl C, Poplin R, del Angel G, Levy-Moonshine A, Jordan T, Shakir K, Roazen D, Thibault J, Banks E, Garimella K, Altshuler D, Gabriel S, DePristo M. From FastQ Data to High-Confidence Variant Calls: The Genome Analysis Toolkit Best Practices Pipeline. *Current Protocols in Bioinformatics*, 2013;43:11.10.1-33.

[29] International HapMap Consortium. The International HapMap Project. *Nature*, 2003;426(6968):789-796.

[30] Strong SP, Koberle R, de Ruyter van Steveninck RR, Bialek W. Entropy and Information in Neural Spike Trains. *Phys. Rev. Lett.*, 1998;80:197.

[31] Howie BN, Donnelly P, Marchini J. A flexible and accurate genotype imputation method for the next generation of genome-wide association studies. *PLoS Genetics*, 2009;80:5(6):e1000529.

[32] Howie BN, Marchini J, Stephens M. Genotype imputation with thousands of genomes. *G3: Genes, Genomics, Genetics*, 2011;1(6):457-470.

[33] Howie BN, Fuchsberger C, Stephens M, Marchini J, Abecasis GR. Fast and accurate genotype imputation in genome-wide association studies through pre-phasing. *Nature Genetics*, 2012;44(8):955-959.

[34] Lander ES, Waterman MS. Genomic mapping by fingerprinting random clones: a mathematical analysis. *Genomics*, 1988;2(3):231-239.

[35] Rasmussen CE, Williams CKI. Gaussian Processes for Machine Learning. *MIT Press*, 2006;ISBN 0-262-18253-X.

[36] Dwork C. Differential Privacy: A Survey of Results. *Springer Berlin Heidelberg*, 2008;Theory and Applications of Models of Computation. Lecture Notes in Computer Science. pp. 1-19

[37] Conesa A, Madrigal P, Tarazona S, Gomez-Cabrero D, Cervera A, McPherson A, Szczesniak M, Gaffney D, Elo LL, Zhang X, Mortazavi A. A survey of best practices for RNA-seq data analysis. *Genome Biol.*, 2016;17:13-14.

S. Fienberg, A. Slavkovic, and C. Uhler. Privacy preserving GWAS data sharing. In ICDM, pages 628635, 2011.

A. Johnson and V. Shmatikov. Privacy-preserving data exploration in genome-wide association studies. In KDD, pages 10791087, 2013.

F. Yu, S. E. Fienberg, A. B. Slavkovi, and C. Uhler. Scalable privacy-preserving data sharing methodology for genome-wide association studies. Journal of Biomedical Informatics, 2014.

Irit Dinur and Kobbi Nissim. 2003. Revealing information while preserving privacy. In Proceedings of the twenty-second ACM SIGMOD-SIGACT-SIGART symposium on Principles of database systems (PODS '03). ACM, New York, NY, USA, 202-210.

# List of Figures

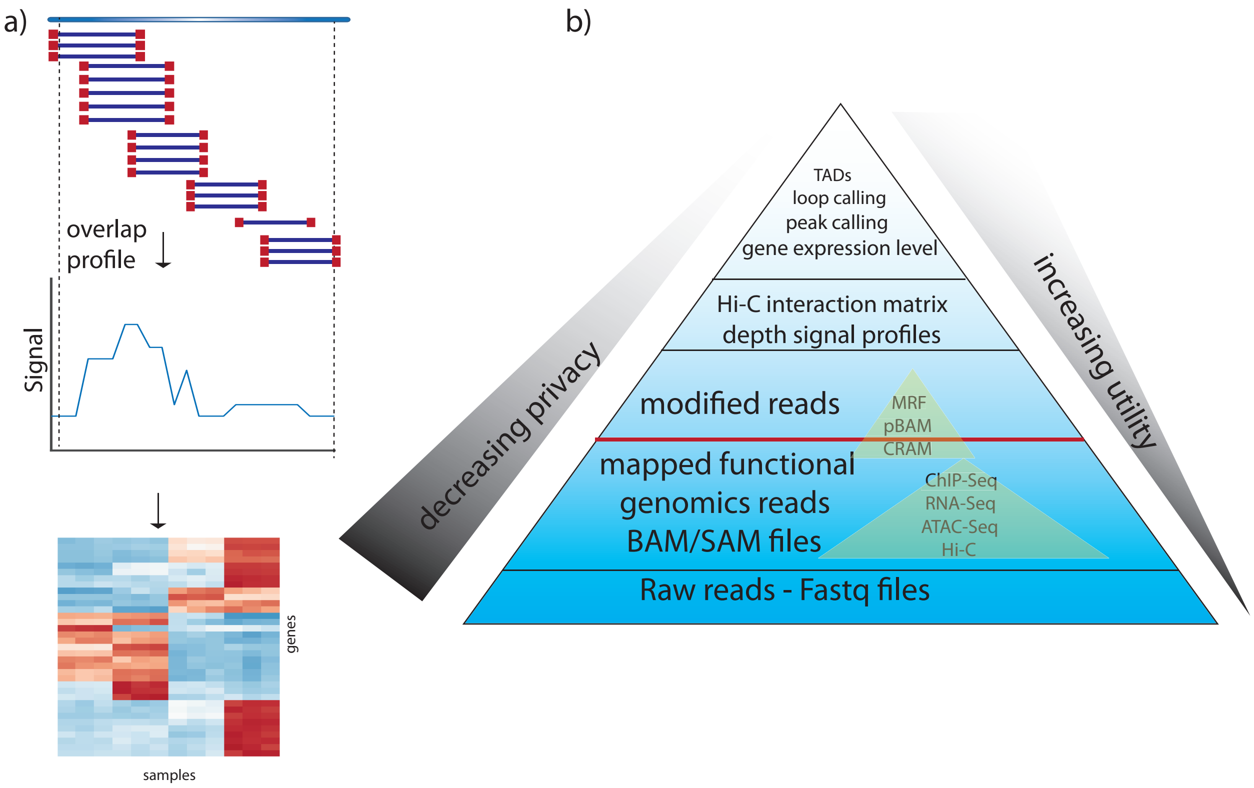

Figure 1: **Schematic of data types from functional genomics experiments.** (**a**) The flow for RNA-Seq data processing from mapped reads to the gene quantifications. (**b**) Different layers of produced data from RNA-Seq pipeline. Red line denotes the set point, where privacy and utility trade-off balanced.

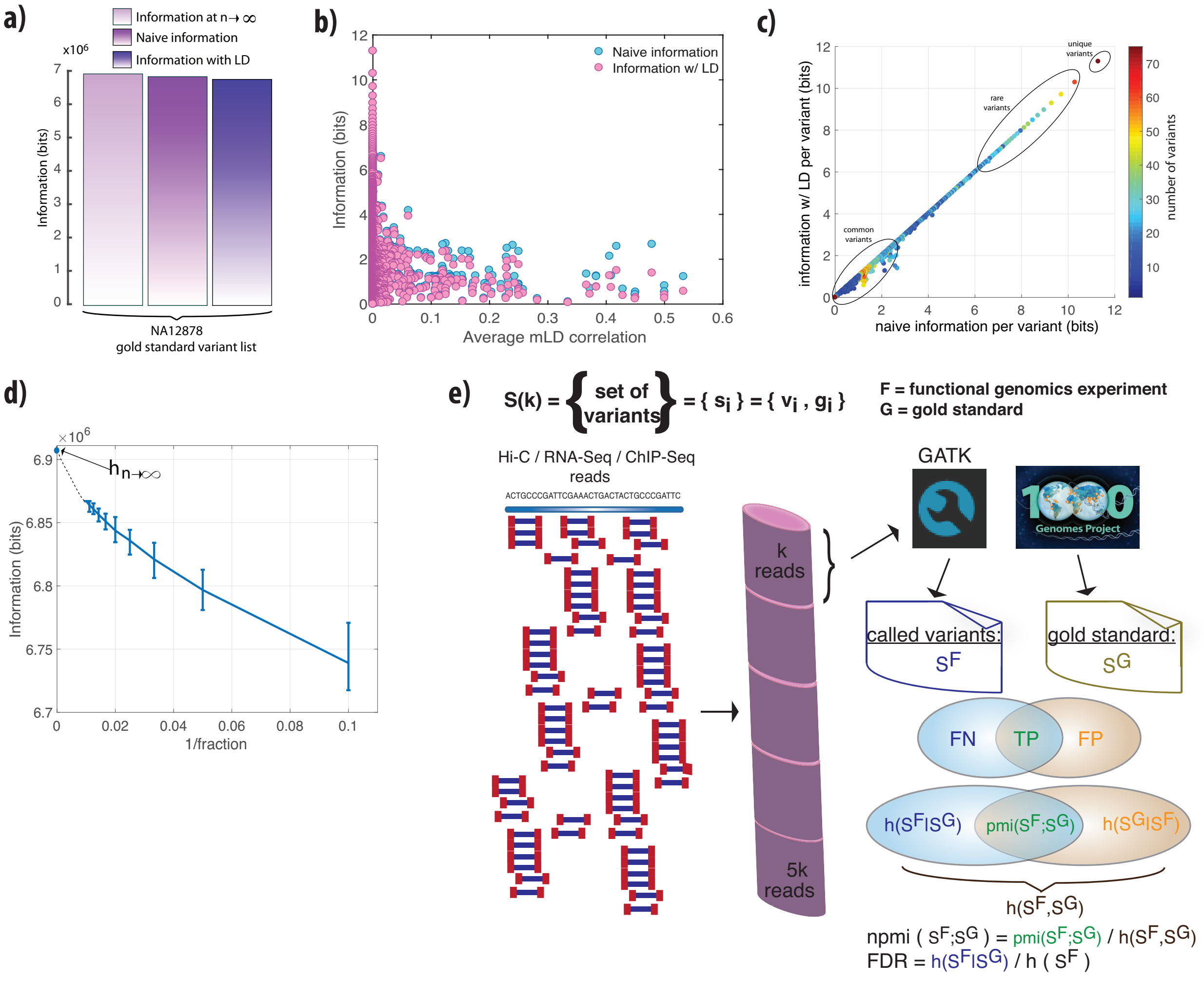

Figure 2: **Comparison of naive information measure with information with LD consideration and sample size correction.** (**a**) Difference between the naive information, information with LD consideration and extrapolated information when population size is infinite. (**b**) The maximum LD score for each variant are averaged over per information and plotted against information. Highly informative variants do not exhibit difference when information is calclated sing naive approach vs. with LD consideration. (**c**) Naive information vs. information with LD consideration per each variant in an LD block. Only low information variants show slight difference between two approaches. (**d**) Naive information vs. inverse fraction of the data sampled from the 1000 genomes population. $y$-intercept is extrapolated from the fitted curve and denotes the information when the population size is infinite. Error bars are calculated using 100× bootstrapping. (**e**) The process of sampling reads from functional genomics experiments for the calculation of pointwisw mutual information between 1000 genomes gold standard variants for NA12878 in different coverages.

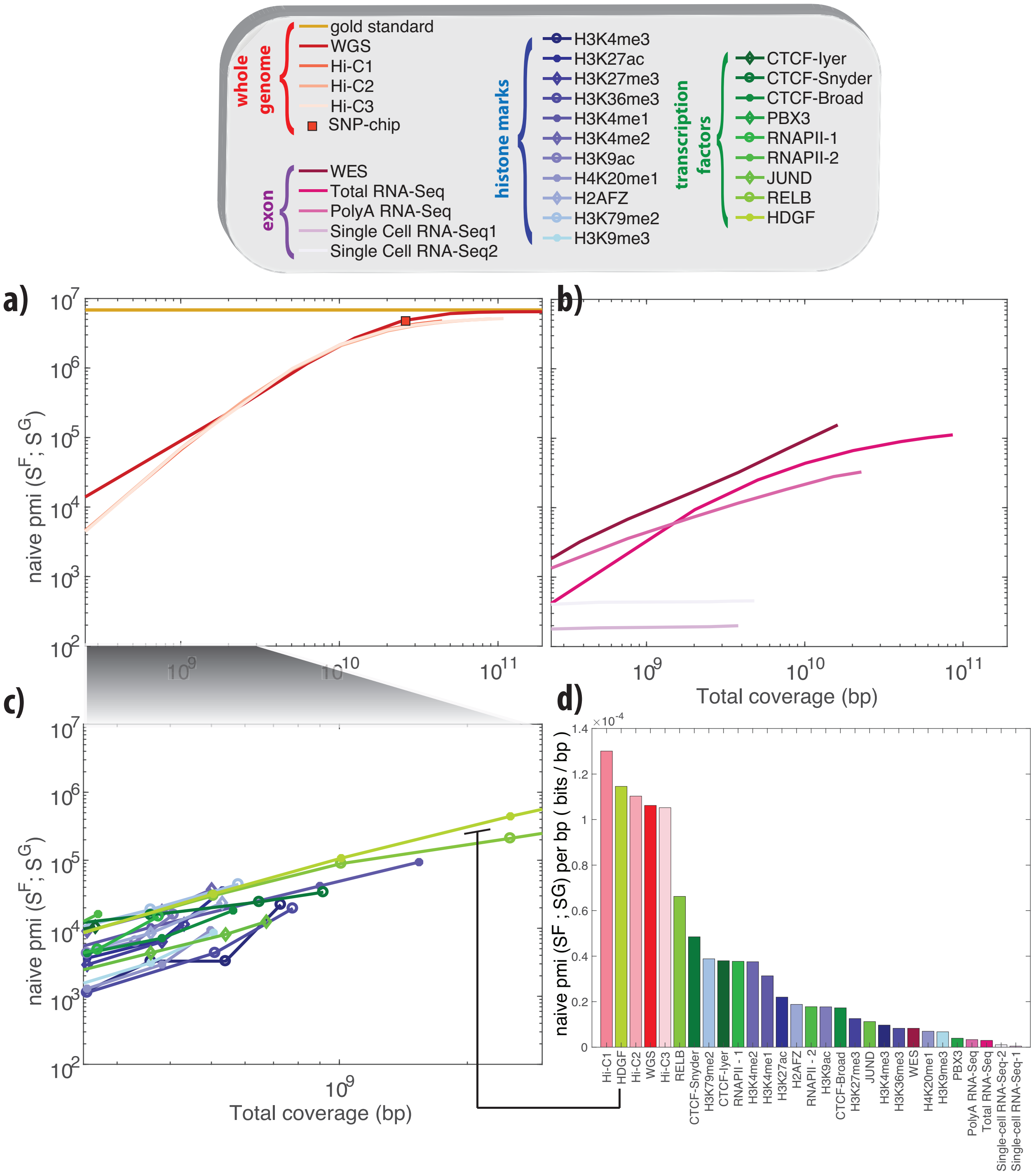

Figure 3: **The pointwise mutual information calculated for 24 different functional genomics assays and WGS, WES and SNP ChIP data using NA12878 1000 genomes variants as gold standard.** (**a**) The pmi values for WGS and three different primary Hi-C experiments plotted at different coverages. The information contents of the gold standard (1kG in blue) and SNP ChIP (in pink) are added for comparison. (**b**) The pmi values for 20 different ChIP-Seq experiments targeting histone modifications and transcription factor binding plotted at different coverages. (**c**) The pmi values for WES, total RNA-Seq, polyA RNA-Seq and single-cell RNA-SEq from two different cells plotted at different coverages. (**d**) The pmi values per basepair plotted using the mean of all the ratios between the pmi and the corresponding coverage.

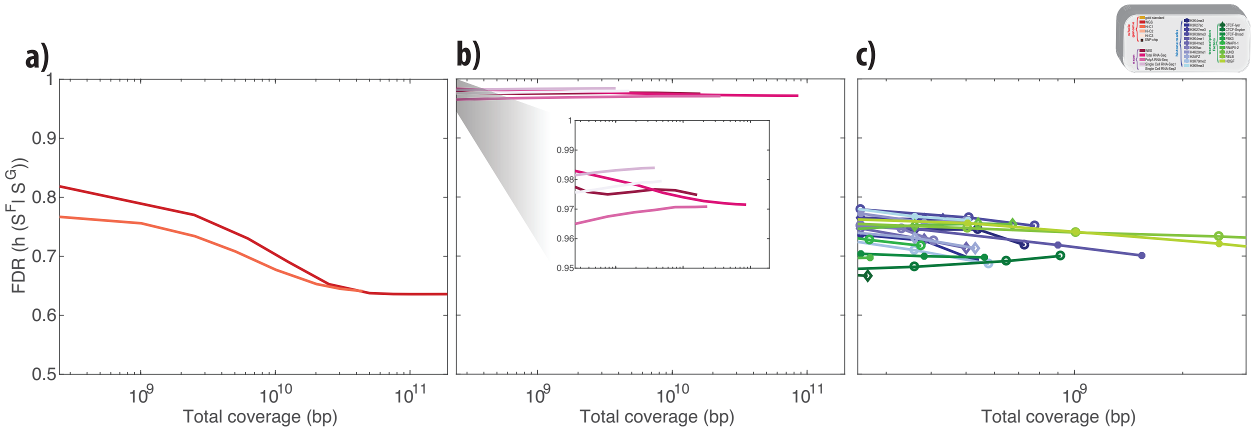

Figure 4: **False discovery rate of functional genomics experiments at different coverages** (**a**) FDR comparison for Hi-C and WGS data at different sampled coverages. (**b**) FDR comparison for different ChIP-Seq experiments at different coverages. (**c**) FDR comparison for WES and different RNA-Seq experiments.

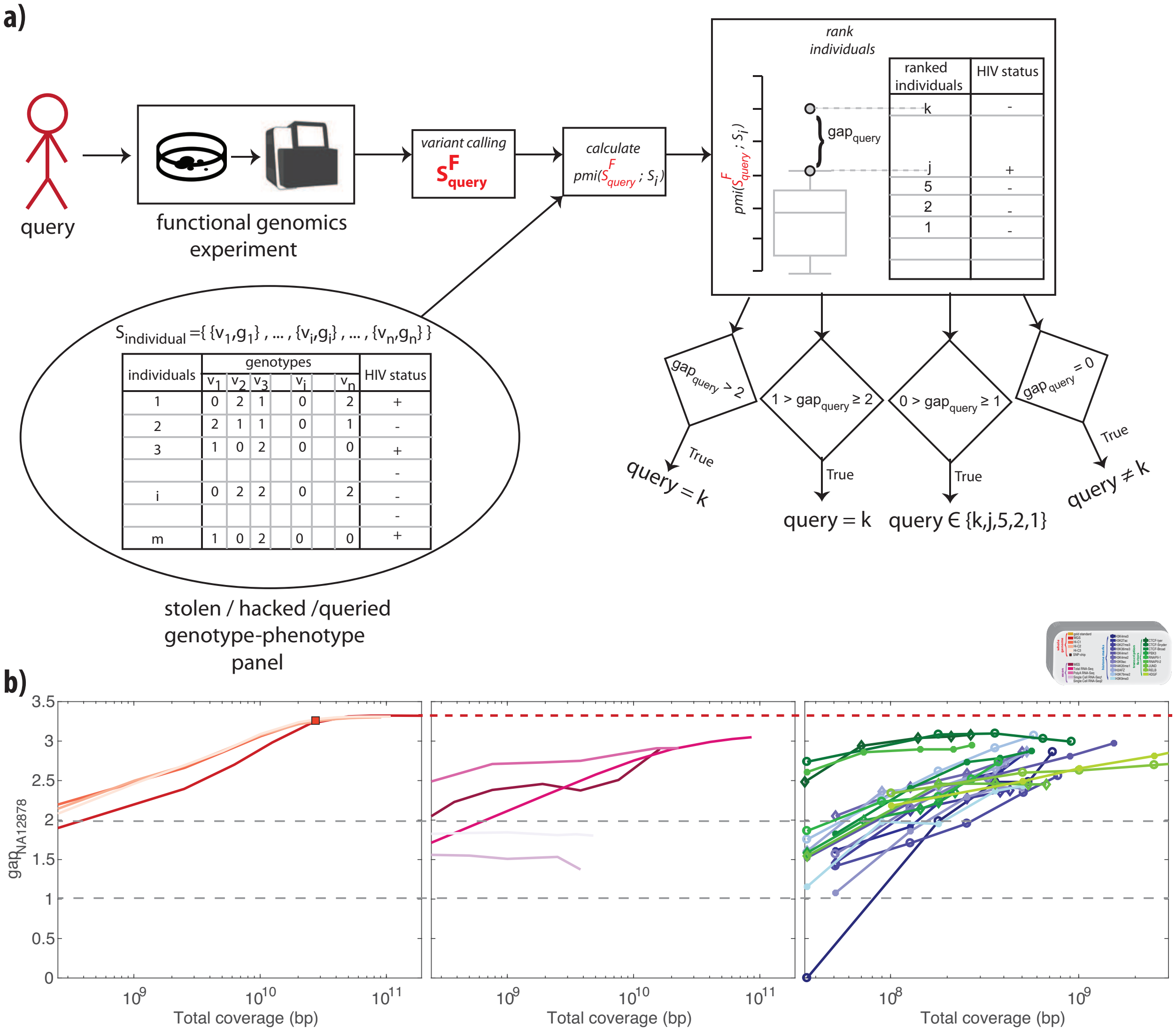

| individuals | genotypes | | | | | | | HIV status |
|---|---|---|---|---|---|---|---|---|
| | $v_1$ | $v_2$ | $v_3$ | | $v_i$ | | $v_n$ | |
| 1 | 0 | 2 | 1 | | 0 | | 2 | + |
| 2 | 2 | 1 | 1 | | 0 | | 1 | - |
| 3 | 1 | 0 | 2 | | 0 | | 0 | + |
| | | | | | | | | - |
| i | 0 | 2 | 2 | | 0 | | 2 | - |
| | | | | | | | | - |
| m | 1 | 0 | 2 | | 0 | | 0 | + |

Figure 5: **Illustration of a linking attack and the accuracy of linking.** (**a**) The publicly available ananoymized reads from functional genomics experiments contains a set of variants and HIV status for the sample that the functional genomics experiment was performed at increasing coverages. The panel of genotypes contains the variants and associated genotypes for *m* individuals. The attacker links the inferred variants and genotypes to the panel of genotypes by using the best matched pointwise mutual information. The linking potentially reveals the HIV status for the linked individual. (**b**) Comparison of *gap* for NA12878 at different coverages for Hi-C and Total/PolyA RNA-Seq reads. WGS and SNP-ChIP are also added for comparison. (**c**) Comparison of *gap* for NA12878 at different coverages for 20 different ChIP-Seq experiments. (**d**) Comparison of *gap* for NA12878 at different coverages for single-cell RNA-Seq experiments.

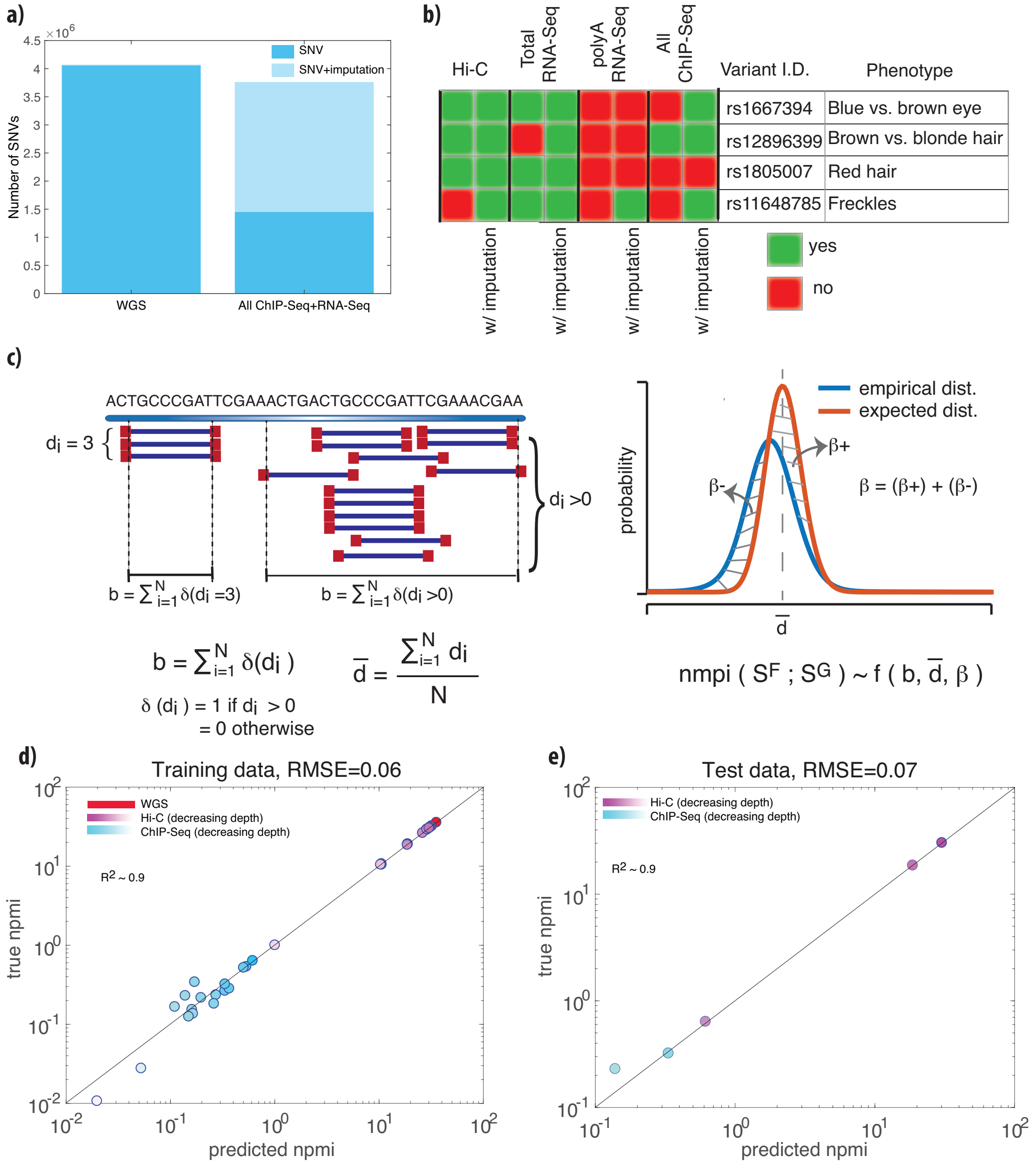

Figure 6: **Individual's genome can be approximated and sensitive phenotypes can be inferred from publicly available data by imputation and a theoretical framework for prediction of amount of leaked data** (**a**) Number SNVs called from WGS data and all of the ChIP-Seq and RNA-Seq data together with and without imputation. (**b**) Variants associated with physical traits and if they present in the called variants from different functional genomics experiments before and after imputation. (**c**) Features of the theoretical framework - write more. (**d**) Accuracy of fitted model on training set- write more (**e**) Accuracy of fitted model on test set - write more

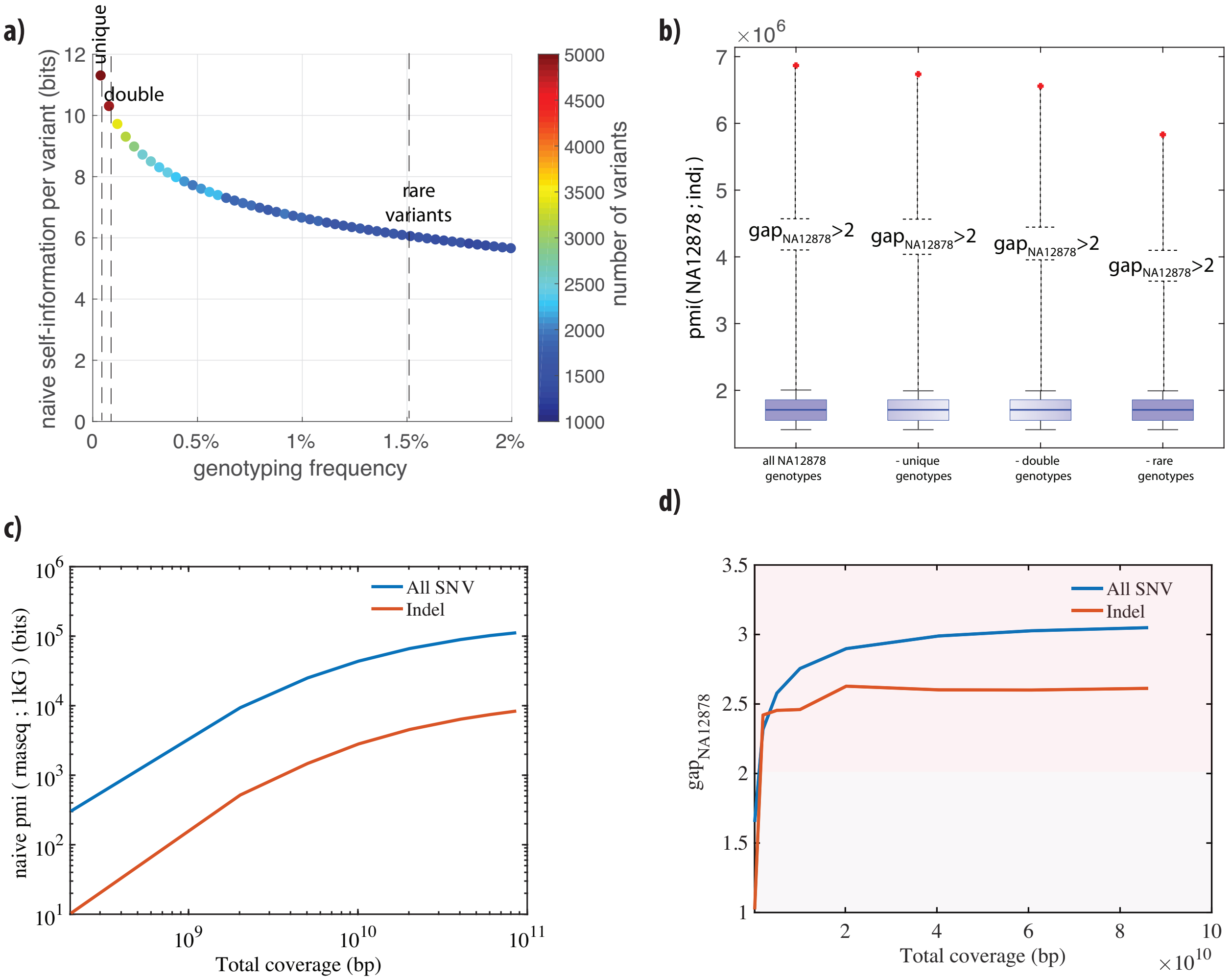

Figure 7: **Removal of rare variants and linking** (**a**) Information of the variant before and after addition of NA12878 to the population. We iteratively removed variants from the set as (I) only the variants that is only NA12878 specific, (II) the variants that have an information of 11 or higher bits after removal of NA12878 from the population, (III) the variants that have an information of 6 or higher bits after removal of NA12878 (**b**) Linking accuracy for every iteration of removal of NA12878 variants from the set. (**c**) Information of all the variants that are called from Total RNA-Seq reads vs. the information of the indels that are called from Total RNA-Seq reads. (**d**) Linking accuracy when we consider all the variants that are called from Total RNA-Seq rads vs. the linking accuracy when we consider only indels called from Total RNA-Seq reads.

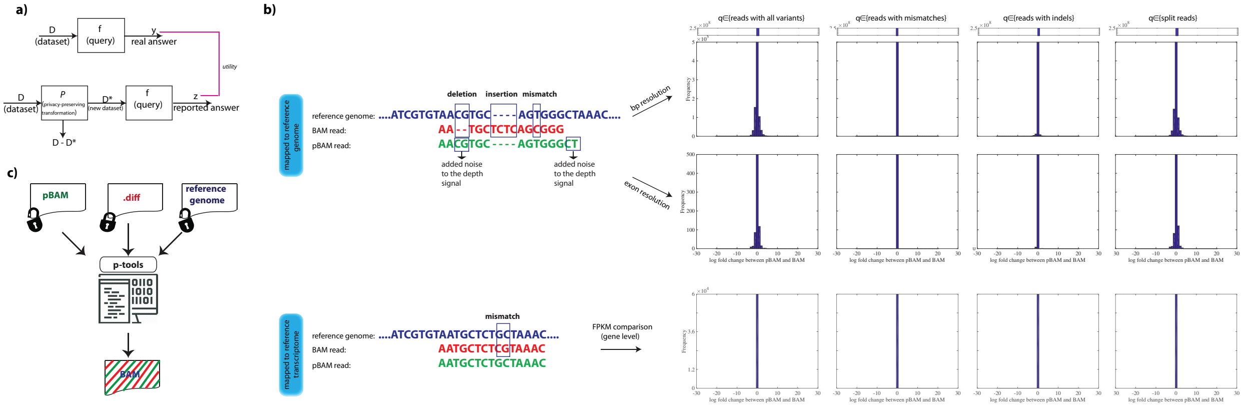
a)
D
(dataset)
f
(query)
y
real answer
utility
D
(dataset)
P
(privacy-preserving transformation)
D*
(new dataset)
f
(query)
z
reported answer
D - D*
b)
mapped to reference genome
deletion
insertion
mismatch
reference genome: ....ATCGTGTAACGTGC----AGTGGGCTAAAC....
BAM read: AA--TGCTCTCAGCGGG
pBAM read: AACGTGC----AGTGGGCT
added noise to the depth signal
added noise to the depth signal
bp resolution
exon resolution
mapped to reference transcriptome
mismatch
reference genome: ....ATCGTGTAATGCTCTGCTAAAC....
BAM read: AATGCTCTCGTAAAC
pBAM read: AATGCTCTGCTAAAC
FPKM comparison (gene level)
q∈(reads with all variants)
q∈(reads with mismatches)
q∈(reads with indels)
q∈(split reads)
Frequency
log fold change between pBAM and BAM
c)
pBAM
.diff
reference genome
p-tools
BAM

Figure 8: **Privacy-preserving file formats for mapped reads** (**a**) The generation of public pSAM and private .diff files. (**b**) Schematic of how to go between pBAM and BAM formats by utilizing the human reference (**c**) Comparison of nmber of reads for each basepair in the original SAM file and the distorted pSAM file. Noise is mostly introduced to basepairs with low depth. (**d**) Comparison of nmber of reads for each exon in the original SAM file and the distorted pSAM file. Noise is mostly introduced to exons with low expression.